Geosci. Instrum. Method. Data Syst. Discuss., https://doi.org/10.5194/gi-2018-8
Manuscript under review for journal Geosci. Instrum. Method. Data Syst.
Discussion started: 23 March 2018
© Author(s) 2018. CC BY 4.0 License.

Geoscientific Instrumentation Methods and Data Systems Discussions
Open Access
EGU

Links between annual surface temperature variation and land cover heterogeneity for a boreal forest as characterized by continuous, fibre-optic DTS monitoring

Kazuyuki Saito[1,2], Go Iwahana[2], Hiroki Ikawa[3], Hirohiko Nagano[2,4], Robert Busey[2]

[1]Japan Agency for Marine-Earth Science and Technology, Yokohama, 236-0001, Japan
[2]International Arctic Research Center, University of Alaska Fairbanks, Fairbanks, Alaska 99775, U.S.A.
[3]National Institute for Agro-Environmental Sciences, Tsukuba, 305-8604, Japan
[4]Japan Atomic Energy Agency, Tokai, 319-1195, Japan

Correspondence to: Kazuyuki Saito (ksaito@jamstec.go.jp)

Abstract. A fibre-optic DTS (distributed temperature sensing) system using Raman-scattering optical time domain reflectometry was deployed to monitor a boreal forest research site in the interior of Alaska. Surface temperatures range between -40º C in winter to 30º C in summer at this site. In parallel experiments, a fibre-optic cable sensor system (multi-mode, GI50/125, dual core; 3.4 mm) monitored at high-resolution (0.5-metre intervals every 30 minutes) ground surface across the landscape and, at several points a high resolution vertical profile from the upper subsurface to a meter above.. The total cable ran 2.7 km with about 2.0 km monitoring a horizontal surface path. Sections of the cable sensor were deployed in vertical coil configurations (1.2 m high) to measure vertical temperature profiles from the ground up at 5-mm intervals. Measurements were collected continuously over a two year interval from October, 2012 to October, 2014. Vegetation of the overall site (Poker Flat Research Range) consists primarily of black spruce underlain by permafrost. Land cover types within the study area were classified into six descriptive categories: relict thermokarst lake, open moss, shrub, deciduous forest, sparse conifer forest, and dense conifer forest. The horizontal temperature data exhibited spatio-temporal patterns within the observed diurnal and seasonal variation. Differences in snow pack evolution and insulation effects co-varied with the land cover types. The apparatus used to monitor vertical temperature profiles generated high-resolution (c. 5 mm) data for air column, snow cover, and ground surface. This research also identified several technical challenges of deploying and maintaining a DTS system in sub-arctic environments.

1 Introduction

Under the current climate conditions, boreal forest regions function as major carbon sinks (IPCC, 2013; Euskirchen et al., 2006; Piao et al., 2008; Ohta et al., 2008). Taiga regions however can show considerable variation (heterogeneity) in land

© Author(s) 2018. CC BY 4.0 License.

cover, hosting both dense and sparse forests, shrubs, grasses, open mosses, and bare ground. Depending on their structural features and seasonal variation, each of these land cover types behaves differently in terms of energy, mass, and momentum exchange. These factors include presence of and variation in different forms of canopy, aerodynamic and radiative characteristics, phenology and snow pack, all of which can influence geothermal flux, subsurface physical conditions, and microbial activity (Euskirchen et al., 2006; Pomeroy et al., 2008; Essery et al., 2009; Rutter et al., 2009; Kasurinen et al., 2014; Ikawa et al., 2015; Purdy et al., 2016). For boreal forests, surface and subsurface condition are critical causal variables, especially in terms of their spatio-temporal variation. Surface heterogeneity can also exert non-linear influence on energy, mass, and momentum exchange with the atmosphere (Vrese et al., 2016; Sellers, 1999). In-situ field measurements can help quantify spatio-temporal temperature patterns and help constrain numerical eco-climatic models for taiga regions. Data like that presented and interpreted below thus offer specific empirical information about taiga environments and contribute to larger-scale predictions concerning impacts of Earth's warming climate (e.g., Beer et al., 2007; Sato et al., 2016).

Distributed temperature sensing (DTS) systems perform multi-sensor monitoring of an area using a fibre-optic cable configuration and Raman scattering techniques. Developed in the 1980s and improved thereafter, DTS was initially used in built environments, providing fire detection for example in industrial complexes or power plants (Dakin et al., 1985; Dyer et al., 2012; Soto et al., 2016). The technique was subsequently adapted for hydrological and geophysical research seeking to measure temperature variation in natural environments (Selker et al., 2006a, 2006b; Tyler et al., 2009; Thomas et al., 2012; Lutz et al., 2012). The research described here represents the first time the method has been used to study a boreal forest. Large seasonal variation in ambient temperatures (from -40º C in winter to 30º C in summer) and other conditions (persistent snow cover with deep hoar or ice layers, freeze / thaw cycles) that characterize interior, continental boreal forests recommend these environment to DTS monitoring, which can provide continuous, high resolution data. The data described here include temperature variation and snow pack evolution that reflect the heterogeneous land cover of the boreal forest, and a high resolution vertical profile from the upper subsurface to a meter above.

Section 2 describes the research site and methodology. Section 3 describes results for the horizontal (sections 3.1, 3.2) and vertical (section 3.3) temperature data from the two-year experiment. Section 4 considers technical challenges of using DTS systems in sub-arctic environments and section 5 summarizes the study.

2 Methodology

2.1 Site

The Poker Flat Research Range (65˚07'24" N, 147˚29'15" W, 210 m a.s.l.) is a research facility managed by the University of Alaska Fairbanks (UAF) and located in Interior Alaska, about 50 km northeast of Fairbanks (Fig. 1). The general area is part of a discontinuous permafrost zone but the site itself is underlain by permafrost with active layer thickness of about 50 to 150 cm (Nakai et al., 2013). The research site includes an observation tower built in 2010 as part of a collaboration (known as JICS) between the Japan Agency for Marine-Earth Science and Technology (JAMSTEC) and UAF's International Arctic

© Author(s) 2018. CC BY 4.0 License.

Research Center (IARC) (Sugiura et al., 2011; Nakai et al., 2013; Ikawa et al., 2015 ; Nagano et al., 2018). The JICS observation tower was used to discretely measure air temperature at 1.5-m height, downward short-wave radiation measurements at 16-m height (tower top), and snow depth using an ultra-sonic sensor. The data from these sources were integrated into 30-minute intervals prior to analysis. Measurements were conducted for two years from October 13, 2012 to October 13, 2014.

A ~2.7 km fibre-optic cable was installed at the site (black line in Fig. 2a). The line traversed an arcuate, 2 km long path and included five different stations (numbered 1-5) consisting of vertical temperature sensing apparatus (see Sect. 2.2). The site's dominant vegetation type is black spruce but locally, the site exhibits considerable variation in surface conditions and vegetation types (see Fig. 2a). We classified land cover into six descriptive categories by applying a supervised classification algorithm (Maximum Likelihood) to RGB aerial imagery collected on September 4, 2012. Land cover designations included relict thermokarst, lake/bare ground, open moss, shrub, deciduous forest, sparse conifer forest, and dense conifer forest. The Majority Filter tool (ArcGIS 10.3) was applied to reduce speckle noise prior to classification. Figure 2b shows the occurrence frequencies of the six land cover types along the length of the cable.

Figure 2c shows land cover type associations along with radiative and structural canopy characteristics for each measurement segment (~50-cm intervals) along the cable. The Normalized Difference Vegetation Index (NDVI) was derived from a GeoEye1 image taken on September 25, 2010. The canopy rate, the upper sight ratio covered by vegetation canopy when projected on a hemisphere, was calculated from a series of semi-spherical pictures taken at a height of 30 cm for every 70 cm along the cable by a THETA fish-eye camera (RICOH, Inc. Cylindrical projection). Ellipses are colour-coded for each land cover type and drawn with radii representing the standard deviation in canopy rate (horizontal) and NDVI (vertical).

Figures 2d - 2i shows typical ambient conditions for each land cover type. Relict thermokarst lake areas (Fig. 2d) for example include grassy depressions or flats once occupied by lakes formed by subsidence due to melting of ground ice from permafrost. This category also includes easily discernible bare grounds cleared by humans. Open moss areas (Fig. 2e) consist of open spaces covered by moss (mainly sphagnum moss, *Sphagnum fuscum*, and feather moss, *Hylocomium splendens*) or lichens, with trees absent. Shrub areas (Fig. 2f) are covered dwarf to tall shrubs. Deciduous forest land cover (Fig. 2g) consists of mixed forests with deciduous (birch, aspen, willow, etc.), and conifer (black spruce, *Picea mariana*, and white spruce, *Picea glauca*) species. The sparse conifer (Fig. 2h) and dense conifer (Fig. 2i) forest land cover types are occupied by spruces of varying density. The forest floors are mainly covered by moss with occasional shrubs where trees are sparse.

2.2 Methods

The fibre-optic DTS (distributed temperature sensing) system deployed in this study used Raman-scattering, optical time domain reflectometry to measure temperatures along the cable (Dakin et al., 1985). Scattering of incident photons from a laser pulse within the optical fibre (SiO_2) includes back scatter at different frequencies (Raman scattering). The system can record intensity ratios within the scattering (i.e., Stokes and Anti-Stokes peaks). The latter peak is highly sensitive to the temperature

© Author(s) 2018. CC BY 4.0 License.

of the medium while the former is not (Fig. 3). The location of the temperature detected is determined by the travel time (i.e., optical time domain reflectometry). Measurements were performed in dual (looped) mode wherein the laser pulse is emitted from alternate channels at each end of the cable. Calibration was performed at 0º C using a 10-m segment of the cable.

This study used a 2.7 km long fibre-optic cable (multi-mode, GI50/125, dual core; 3.4 mm, S2002A, manufactured by BRUGG, Switzerland) installed horizontally over a 2.0 km surface path (referred to as the horizontal section). Portions of the cable were also coiled around PVC tubes (effective outer diameter of 11.5 cm, and length of about 120 cm). The tubes were vertically embedded in the ground to half of their length (60 cm deep) at five stations numbered 1-5 (Fig. 2a) along the horizontal pathway. Figure 2i shows a tube being installed while Figure 2e shows a tube in operation. One loop of the coil measured about 36 cm so that three loops (*c.* 1 m) corresponded to two measurement segments (a segment = 50 cm). This gave an effective vertical resolution of about 5 mm. Temperature data from the embedded tubes are referred to as the vertical sections. Temperatures were also measured at 50 cm intervals along horizontal (non-coiled) sections of the cable. Measurements taken every 10 seconds were integrated over 30 minute intervals to reduce measurement error and noise. The experiment operated continuously over a two-year interval from October, 2012 to October, 2014, except for several disruptions due to cable or power supply failure. Temporal monitoring was referenced to Alaskan Standard time (UTC - 9 hours).

3 Results

Figure 4 shows an example of data averaged over a 24 hour period (December 1, 2013) along the horizontal section. The daily average tower air temperature (measured at 1.5 m) was -32.5º C and daily mean snow depth was 23.5 cm. Downward spikes corresponds to those parts of the cable exposed above the upper surface of the snow pack (minimum temperature was -32.6º C while the maximum temperature was +1.0º C). For this season, this temperature difference of more than 30º C is likely due to combinations of insulation by snow pack, and the saturation and unfrozen moisture content of the near-surface soils.

3.1 Diurnal and seasonal variation

Figure 5 shows DTS measurements for the six different land cover types. Diurnal and seasonal variation in surface temperatures indicate the influence of both microclimates and micro-environments. Land cover types co-vary with surface conditions, canopy structure, and temporal patterns at each location. Figure 5 shows diurnal and seasonal temperature variation for each land cover type over the two-year period. Daily maximum and minimum temperatures (both in blue), and daily average temperatures (dark blue) from the DTS data are plotted with the JICS tower (1.5 m high) air temperatures (orange and red, respectively). The daily climatology is overlaid in black. The blank periods (e.g., days 10-146, 165-191, and 261-295) denote values missing from either DTS or tower datasets. At the beginning of the 2012-2013 winter, the cable was unexpectedly severed at a point close to the DTS equipment. This event interupted data collection along most of the cable section until the

© Author(s) 2018. CC BY 4.0 License.

cable could be spliced back together, after the snow melt. Section 4 discusses difficulties of using DTS equipment in taiga environments.

For the winter period (days 400-550), open moss (Fig. 5b; canopy rate=0.29, NDVI=0.592), shrub (Fig. 5c; canopy rate=0.34, NDVI=0.515), and both conifer forests types (sparse conifer in Fig. 5e; canopy rate=0.35, NDVI=0.531, and dense conifer in Fig. 5f; canopy rate=0.43, NDVI=0.495) show relatively minor variation in diurnal and daily temperatures. By contrast, thermokarst lake (Fig. 5a; canopy rate=0.46, NDVI=0.404) and deciduous forest (Fig. 5d; canopy rate=0.43, NDVI=0.239) land cover types show greater variability in daily temperatures and resume pronounced diurnal cycles relatively early on, after day 480. The ground cover for the latter two cases includes grass or limited floor vegetation, both of which are of lesser surface roughness (Figs. 2d and 2g). Differences between the two groups stem primarily from differences in snow pack characteristics. Snow pack tends to be thinner and effectively redistributed or blown by wind for the latter land cover types. Grasses are also prone to form void space between snow pack and the ground surface. Snow pack variation is further described in section 3.2 below.

In summer time (days 220 to 350, and 570 to 700), dense conifer forest exhibited daily surface temperature ranges (DTS data) less than those observed for the air column (tower observations). By contrast, open moss, shrub, and sparse forest types showed daily surface temperature ranges that were greater than those of the overlying air column. The grassy relict lake and deciduous forest land cover types showed an intermediate response. These tendencies likely reflect the openness of the canopy (or vegetation) cover above at the land surface (i.e., how much solar and longwave radiation reach the sensor cable), as well as local albedo of different surfaces (i.e., how much the ground surface of different land cover types reflects back). Figures 6a-6c show daily values (i.e., maximum, minimum, and average) for the DTS temperature anomaly relative to the corresponding tower values for days without snow cover or missing values. Results were aggregated into four groups based on daily cloudiness, as defined by the percentage of daily total downward solar radiation between the tower (at 16-m height) and the top of the atmosphere. A box-and-whisker plot shows maximum values (100%-ile) as the top of the upper error bar, 75%-ile as the upper edge of the box, 50%-ile as the colour-coded bar, 25%-ile as the lower edge of the box, and the minimum (0%-ile) as the bottom of the lower error bar. The plot shows uniform, gradual changes in anomaly distributions from sunny days to cloudy days (Figs. 6a-6c). The size of anomaly dispersions for each land cover type (represented by the total span of the whiskers) decreases with increasing cloud cover, due to clouds' diffusing effects. Daily average temperatures at the surface generally exceed those observed by the JICS tower (at 1.5 m height). Daily maximum values appear to contribute to this effect more than do daily minimum values. The latter (daily minimum) values are closer to the tower-observed values. Among different land cover types, open moss and deciduous forest tend to give higher daily maximum and lower daily minimum anomalies.

Figures 6d and 6e show phases of diurnal extremes (i.e., exact time of either the original daily maximum or daily minimum temperature) for the DTS (colour-coded bars) and JICS tower (black line) observations, respectively. The daily maximum for surface temperatures (Fig. 6d) obtains two hours before that of the air temperature. Relict thermokarst lake areas (grassy or

© Author(s) 2018. CC BY 4.0 License.

bare grounds) tend to reach to the daily maximum temperature earlier and deciduous forest areas later than other land cover types. For the daily minimum temperature (Fig. 6e), surface and air temperatures are more in-phase with each other. This temperature obtains in the 3rd to 4th hour (3-4 am) slot for a normal daily cycle, or at the 23rd to 24th hour (11-12 pm).

3.2 Spatial snow cover characteristics

As shown in Figure 5, snow pack greatly affects winter-time thermal conditions at the interface between the ground and snow pack. Snow cover on the ground surface strongly influences the radiative and energy budget, the water cycle, and phenology (Sturm et al., 2005; Liston, 1999; Tan et al., 2011; Immerzeel et al., 2010; Jönsson et al., 2010). Seasonal snow pack data (e.g., timing of when / how snow pack accumulates and disappears) is important for interpreting observed temperature values and for constraining energy budgets within numerical models. Snow pack is affected by the land cover types, which can amplify contrasting conditions (Liston, 1999, 2004; Sturm et al., 2005). Here, we describe how DTS data indicate different trajectories of snow pack evolution (namely, appearance and disappearance) and produce apparent insulation effects for different land cover types.

Figure 7a shows dates of initial snow accumulation (the middle panel) and final disappearance (left and rightmost panels) for each land cover type, as counted from the date shown at the bottom of the respective panel. The presence of a continuous anow cover was defined by whether the daily amplitude in DTS temperatures fell short of 40% of that of JICS tower (1.5 m high) observations. As shown in Figure 7b, this 40% threshold effectively differentiates between snow-free and snow-covered conditions. The overall contrast between accumulation and disappearance dates (Fig. 7a) indicates that accumulation of snow cover tends to begin as spatially coherent and widespread, whereas disappearance of snow pack varies according to local conditions (Liston, 2004; Nitta et al., 2014). Among different land cover types, the majority (denoted by the margin between the 25%-ile and 75%-ile) of grassy (relict thermokarst lakes; blue) and shrubby (shrub; orange) areas vary more widely than do the forest land cover types (greens). Open moss (red) of relatively flat areas shows equal or greater variation than forest land cover types.

Another important geophysical effect of snow cover is the insulation it provides between the atmosphere and land surface. Figure 7b demonstrates this effect by showing the reduction in daily temperature range for the ground surface relative to the air. Open moss land cover shows the most spatially coherent and pronounced reduction. This implies spatial homogeneity in snow pack depth and physical properties (e.g., density, shape and size of snow grain, snow class), which could contribute to similar timing of snow disappearance (Fig. 7a). The strong insulation effect likely results from development of the depth hoar layer by radiative cooling. Relict thermokarst lake areas show high spatial variability in temperature range reduction. Forested land cover showed small reductions regardless of the forest types, possibly due to cooler ambient conditions beneath canopy.

Geosci. Instrum. Method. Data Syst. Discuss., https://doi.org/10.5194/gi-2018-8
Manuscript under review for journal Geosci. Instrum. Method. Data Syst.
Discussion started: 23 March 2018
© Author(s) 2018. CC BY 4.0 License.

Geoscientific Instrumentation Methods and Data Systems Discussions
Open Access
EGU

3.3 Vertical temperature profiles

The fibre-optic cable wrapped around a 120 cm long, PVC tube provided high-resolution vertical temperature profiles for air and snow columns (Fig. 8a-b) at five locations each situated within different land cover types (Fig. 2a). Location #1 was sited in dense forest, #2 in sparse forest, #3 in open moss, #4 in shrub, and #5 in a relict thermokarst lake area. Figures 8c-d show seasonal changes in daily mean temperature and temperature range for station #1, respectively. White areas represent missing values due to either cable disruption or other technical issues. Blue areas in Figure 8d show daily temperature values whose ranges are curtailed either by snowpack (above-ground for the part above the black line) or ground (below the black line). Together with Figure 8c, Figure 8d shows the structure and variation in temperature regimes for the air and/or snow column above-ground and during frozen or thawed subsurface conditions. The original 30-minute data reveals thermal properties of the soil or snow media (i.e., thermal conductivity or diffusivity).

4 Technical challenges

As described above, DTS provides continuous datasets for analysing spatial variability in temperature. Data continuity however depends on functioning fibre-optic cables, uninterrupted power and communication capabilities, which in turn depend on robust equipment performance under harsh and highly variable conditions. This section describes specific technical and environmental challenges identified during our study.

A continuous electrical power supply is critical for remote DTS field data collection. This requirement limits locations where DTS apparatus can be deployed. Even when available, the power system used here was subject to harsh temperature and precipitation conditions. A durable, uninterrupted power supply (UPS) is recommended for future experiments. Fibre-optic cables also pose significant logistical challenges when deployed in remote taiga forest environments. Irregular surface areas with variable moisture and numerous obstacles (such as trees) prevent construction of a simple, protected route for the cable. Deploying a ~3 km long cable from a large wooden spool which, together with the cable weighed more than 50 kg, around barriers and across soggy ground posed significant challenges. We chose a cable with a stainless steel shielding tube, to optimize sensing capabilities but also protect from disruption by animals. The shielding turned out to have suboptimal flexibility (compared to that of woven stainless mesh shielding), which led to kinking and even breaking during installation. The tube-shielded cable was also too inflexible for the irregular ground surface.

A better future approach to cable routing would be use a smaller, lighter spool and shorter cable, installing the sensor as a series of shorter cable segments. A fusion splicer, already necessary for cable repair, could be used to splice shorter segments of cable in the field instead of installation of a single, long cable. Cable splicing and repair requires some training and experience, especially for performing correct core alignment under field conditions. Splicing is also not possible under harsh winter conditions (e.g., -20º C or below), even though the cable and DTS still function at these temperatures.

The DTS system is also vulnerable to cable breaks. Once the cable breaks, it cannot measure temperature beyond that point. If the cable breaks at 1 m of a 1 km cable system, in other words, the remaining 999 m will produce no data. Dual-mode

© Author(s) 2018. CC BY 4.0 License.

measurement (a cable loop connected to two channels at both ends) can prevent total loss of measurements beyond the break, although the resulting single-mode measurements need additional calibration.

5 Summary

We deployed a fibre-optic DTS (distributed temperature sensing) system, which used Raman-scattering, optical time domain reflectometry to measure spatial variation in surface temperatures of a northern forest (taiga) site situated in Interior Alaska. The DTS system consisted of a 2.7 km fibre-optic cable installed on, above or below surface areas represented by a range of different land cover types. The system provided continuous temperature measurements at half-metre resolution and 30 minute intervals. The site, the Poker Flat Research Range (managed by the University of Alaska Fairbanks) is underlain by permafrost and primarily covered by black spruce. Land cover types of the actual study area were classified into six categories: relict thermokarst lake, open moss, shrub, deciduous forest, sparse conifer forest, and dense conifer forest. The DTS system collected data over a two-year period from October, 2012 to October, 2014.

Data from horizontal sections of the DTS system (about 2.0 km of the cable) recorded diurnal and seasonal temperature patterns that varied according to different land cover types and surface conditions. Snow and canopy effects for example were evident in spatio-temporal temperature patterns. Data from vertical sections (cable wrapped around PVC tubes embedded in the ground) recorded air, snow, and ground temperatures at high resolution (~5 mm).

The DTS system proved operable and useful for geophysical investigations in the harsh taiga environment, which experiences annual temperature ranges of -40º C to 30º C. However, the system also demonstrated technical challenges of continuous temperature measurements in this environment. Future research will continue to optimize DTS systems for geoscientific research in taiga areas and other harsh environments.

Data accessibility

The DTS measurement data analysed in this paper along with attributional information are archived and accessible at the International Arctic Research Center (IARC) Data Archive of the University of Alaska Fairbanks (http://climate.iarc.uaf.edu/geonetwork/srv/en/main.home?uuid=60804e98-a0d5-4bcc-ab70-5d47af2b50ca).

Author contribution

KS designed and prepared the experiment. All authors deployed the equipment and maintained the measurement system. KS prepared the manuscript with contributions from all co-authors.

© Author(s) 2018. CC BY 4.0 License.

Acknowledgments

This study was conducted as a part of JAMSTEC-IARC Collaboration Study (JICS). This work was partially supported by the Program for Risk Information on Climate Change (SOUSEI Program), the Integrated Research Program for Advancing Climate Models (TOUGOU program), and the Arctic Challenge for Sustainability (ArCS) program, the Japanese Ministry of Education, Culture, Sports, Science, and Technology, and by the Environmental Research and Technology Development Fund 2-1605 of the Japanese Ministry of Environment and Environmental Restoration and Conservation Agency. Authors gratefully acknowledge assistance from K. Noguchi, R. O'ishi, S. Matsumura, T. Nakai, Y. Igarashi, and L. Hess in installing the fibre-optic cables at the PFRR site, and NK Systems Limited for advices and guidance on the DTS settings and operations.

References

Beer, C., Lucht, W., Gerten, D., Thonicke, K. and Schmullius, C.: Effects of soil freezing and thawing on vegetation carbon density in Siberia: a modeling analysis with the Lund–Potsdam–Jena dynamic global vegetation model (LPJ-DGVM). Glob. Biogeochem. Cycle, 21, GB1012, 2007.

Dakin, J. P., Pratt, D. J., Bibby, G. W., and Ross, J. N.: Raman temperature sensor using a semiconductor light source and detector, Electronics Letters, 21(13), 569-570, 1985.

de Vrese, P., Schulz, J.-P., Hagemann, S.: On the Representation of Heterogeneity in Land-Surface–Atmosphere Coupling. *Boundary-Layer Meteorol*., 160, 157–183, 2016.

Dyer, S. D., Tanner, M. G., Baek, B., Hadfield, R. H., and Nam, S. W.: Analysis of a distributed fiber-optic temperature sensor using single-photon detectors, Optics Express, 20(4), 3456-3466, 2012.

Essery, R. L. H., Rutter, N., Pomeroy, J., Baxter, R., Staehli, M., Gustafsson, D., Barr, A., Bartlett, P., and Elder, K.: SnowMIP2: An evaluation of forest snow process simulations. Bulletin of the American Meteorological Society, 90, 1120 - 1135, doi:10.1175/2009BAMS2629.1, 2009.

Ikawa, H., Nakai, T., Busey, R.C., Kim, Y., Kobayashi, H., Nagai, S., Ueyama, M., Saito, K., Nagano, H., Suzuki, R., and Hinzman, L.: Understory CO2, sensible heat, and latent heat fluxes in a black spruce forest in interior Alaska. Agricultural and Forest Meteorology, 214-215, 80-90, 2015.

Immerzeel, W. W., van Beek, L. P. H., and Bierkens, M. F. P.: Climate change will affect the Asian water towers. Science, 328, 1382–1385, doi:10.1126/science.1183188, 2010.

IPCC: Climate Change 2013: The Physical Science Basis, Contribution of Working Group I to the Fifth Assessment Report of the Intergovernmental Panel on Climate Change edited by: Stocker, T. F., Qin, D., Plattner, G.-K., Tignor, M., Allen, S. K., Boschung, J., Nauels, A., Xia, Y., Bex, V., and Midgley, P. M., Cambridge University Press, Cambridge, UK and New York, NY, USA, 1535pp., 2013.

Jönsson, A.M., Eklundh, L., Hellstrom, M., Barring, L., Jonsson P.: Annual changes in MODIS vegetation indices of Swedish coniferous forests in relation to snow dynamics and tree phenology. Remote Sensing of Environment, 114, 2719-2730, 2010.

© Author(s) 2018. CC BY 4.0 License.

Kasurinen, V., Alfresdsen, K., Kolari, P., Mammarella, I., Alekseychik, P., Rinne, J., Vesala, T., Bernier, P., Boike, J., Langer, M., Belelli Marchesini, L., Huissteden, K., Dolman, H., Sachs, T., Ohta, T., Varlagin, A., Rocha, A., Arain, A., Oechel, W., Lund, M., Grelle, A., Lindroth, A., Black, A., Aurela, M., Laurila, T., Lohila A., and Beringer, F.: Latent heat exchange in the boreal and arctic biomes, Global Change Biology, 20, 3439–3456, doi: 10.1111/gcb.12640, 2014.

Liston, G. E.: Interrelationships among Snow Distribution, Snowmelt, and Snow Cover Depletion: Implications for Atmospheric, Hydrologic, and Ecologic Modeling, J. Applied Meteorology, 38, 1474-1487, 1999.

Liston, G. E.: Representing subgrid snow cover heterogeneities in regional and global models. J. Climate, 17, 1381–1397, doi:10.1175/1520-0442(2004)017,1381:RSSCHI.2.0.CO;2., 2004.

Lutz, J. A., Martin, K. A., and Lundquist, J. D.: Using Fiber-Optic Distributed Temperature Sensing to Measure Ground Surface Temperature in Thinned and Unthinned Forests, Northwest Science, 86 (2), doi:10.3955/046.086.0203, 2012.

Nagano, H., Ikawa, H., Nakai, T., Matsushima-Yashima, M., Kobayashi, H., Kim, Y., and Suzuki, R.: Extremely dry environment down-regulates nighttime respiration of a black spruce forest in Interior Alaska. *Agricultural and Forest Meteorology*, 249, 297-309, doi:10.1016/j.agrformet.2017.11.001, 2017.

Nakai, T., Kim, Y., Busey, R.C., Suzuki, R., Nagai, S., Kobayashi, H., Park, H., Sugiura, K., and Ito, A.: Characteristics of evapotranspiration from a permafrost black spruce forest in interior Alaska. Polar Science, 7, 136-148, 2013.

Nitta, T., Yoshimura, K., Takata, K., Oishi, R., Sueyoshi, T., Kanae, S., Oki, T., Abe-Ouchi, A., and Liston, G. E.: Representing Variability in Subgrid Snow Cover and Snow Depth in a Global Land Model: Offline Validation. J. Climate, 27, 3318-3330, doi:10.1175/JCLI-D-13-00310.1, 2014.

Ohta, T., Maximov, T.C., Dolman, A.J., Nakai, T., van der Molen, M.K., Kononov, A.V., Maximov, A.P., Hiyama, T., Iijima, Y., Moors, E.J., Tanaka, H., Toba, T., and Yabuki, H. Interannual variation of water balance and summer evapotranspiration in an eastern Siberian larch forest over a 7-year period (1998-2006). *Agricultural and Forest Meteorology*, **148**, 1941-1953, 2008.

Piao, S. L. et al. Net carbon dioxide losses of northern ecosystems in response to autumn warming Nature, 451, 49-U43, 2008.

Pomeroy, J., Rowlands, A., Hardy, J., Link, T., Marks, D., Essery, R., Sicart, J. E., and Ellis, C.: Spatial Variability of Shortwave Irradiance for Snowmelt in Forests. J. Hydrometeorology, 9, 1482-1490, doi:10.1175/2008JHM867.1, 2008.

Purdy, A. J., Fisher, J. B., Goulden, M. L., and Famiglietti, J. S.: Ground heat flux: an analytical review of 6 models evaluated at 88 sites and globally, J. Geophys. Res. Biogeosci., 121, doi:10.1002/2016JG003591, 2016.

Rutter, N, and 50 others, 2009. Evaluation of forest snow processes models (SnowMIP2). Journal of Geophysical Research, 114, doi:10.1029/2008JD011063Euskirchen, E. S. et al. Importance of recent shifts in soil thermal dynamics on growing season length, productivity, and carbon sequestration in terrestrial high-latitude ecosystems. Global Change Biol. 12, 731–50, 2006.

Sato, H., Kobayashi, H., Iwahana, G. and Ohta, T. Endurance of larch forest ecosystems in eastern Siberia under warming trends. *Eco.l Evol.,* **6**, 5690–5704, 2016.

© Author(s) 2018. CC BY 4.0 License.

Selker, J., van de Giesen, N., Westhoff, M., Luxemburg, W., and Parlange, M. B.: Fiber optics opens window on stream dynamics, Geophys. Res. Lett., 33, L24401, doi:10.1029/2006GL027979, 2006.

Selker, J. S., Thévenaz, L., Huwald, H., Mallet, A., Luxemburg, W., van de Giesen, N., Stejskal, M., Zeman, J., Westhoff, M., and Parlange, M. B.: Distributed fiber-optic temperature sensing for hydrologic systems, Water Resour. Res., 42, W12202, doi:10.1029/2006WR005326, 2006.

Sellers, P.: Modeling and observing land-surface-atmosphere interactions on large scales. *Surv Geophys*, **12**(1–3), 85–114, 1991.

Soto, M. A., Ramírez, J.A., and Thévenaz, L.: Intensifying the response of distributed optical fibre sensors using 2D and 3D image restoration, Nature Communications, 7, 10870, doi:10.1038/ncomms10870, 2016.

Sugiura, K., Suzuki, R., Nakai, T., Busey, R.B., Hinzman, L.D., Park, H., Kim, Y., Nagai, S., Saito, K., Cherry, J.E., Ito, A., Ohata, T., Walsh, J.: Supersite as a common platform for multi-observations in Alaska for a collaborative framework between JAMSTEC and IARC. *JAMSTEC Rep. Res. Dev.*, 12, 61-69, 2011.

Sturm, M., Schimel, J., Michaelson, G., Welker, J. M., Oberbauer, S. F., Liston, G. E., Fahnestock, J., and Romanovsky, V. E.: Winter Biological Processes Could Help Convert Arctic Tundra to Shrubland, BioScience, 55(1):17-26. 2005.

Tan, A., Adam, J. C., and Lettenmaier, D. P.: Change in spring snowmelt timing in Eurasian Arctic rivers. J. Geophys. Res., 116, D03101, doi:10.1029/2010JD014337, 2011.

Thomas, C. K., Kennedy, A. M., Selker, J. S., Moretti, A., Schroth, M. H., Smoot, A. R., Tufillaro, N. B., Zeeman, M. J.: High-Resolution Fibre-Optic Temperature Sensing: A New Tool to Study the Two-Dimensional Structure of Atmospheric Surface-Layer Flow, Boundary-Layer Meteorol., 142, 177–192, doi:10.1007/s10546-011-9672-7, 2012.

Tyler, S. W., Selker, J. S., Hausner, M. B., Hatch, C. E., Torgersen, T., Thodal, C. E., and Schladow, S. G.: Environmental temperature sensing using Raman spectra DTS fiber-optic methods, Water Resour. Res., 45, W00D23, doi:10.1029/2008WR007052, 2009.

© Author(s) 2018. CC BY 4.0 License.

Figure 1: Location of the DTS system installed at the Poker Flat Research Range (PFRR; University of Alaska Fairbanks).

Figure 2: (a) Layout of the fibre-optic cable sensor (black line) installed at the PFRR with stations numbered from 1 to 5 (in white), together with the land cover types designated from satellite images (dark blue: relict thermokarst lake, red: open moss, orange: shrubs, light green: deciduous forest, green: sparse conifer forest, blue: dense conifer forest). (b) Frequency of land cover types along the cable. (c) Scatter plot of surface-measured canopy rate and satellite-derived normalized difference vegetation index (NDVI; GeoEye1 image taken on Sept. 25, 2010). Images show examples of (d) relict thermokarst lake, (e) open moss, (f) shrub, (g) deciduous forest, (h) sparse conifer forest, and (i) dense conifer forest.

Figure 3: Schematics of Raman scattering.

Figure 4: Examples of temperature distribution measured by a horizontal section of the DTS system (daily mean for December 1, 2013).

Figure 5: Typical seasonal variations in daily temperatures for the six land cover types: (a) relict thermokarst lake, (b) open moss, (c) shrub, (d) deciduous forest, (e) sparse conifer forest, and (f) dense conifer forest. Plot shows daily maximum and minimum temperatures from the DTS system (blue lines) and the JICS tower (air column at 1.5 m height; orange lines) along with daily mean values (dark blue for DTS and red for the JICS tower). The black line shows daily climatology. Data span time period after October 13, 2012.

Figure 6: Distributional differences between (a) daily maximum temperatures, (b) daily minimum temperatures, and (c) daily average temperature under different degrees of cloudiness (32 observations for 0-25%, 69 observations for 25-50%, 80 observations for 50-75%, and 5 observations for 75-100%). Lower plots show median maximum (d) and minimum (e) temperature values and frequency (total hours) as measured by DTS for land cover types (colour-coded) compared to corresponding values from the JICS tower (1.5 m height; black-line histogram).

Figure 7: (a) Differences in snow melt (or accumulation) dates for different land cover types for the spring of 2013 (after April 21, 2013), autumn of 2013 (after October 19, 2013), and spring of 2014 (after April 1, 2014). (b) Damping rate for daily temperature range averaged over snow-covered days having continuous measurements (i.e., without missing or interrupted cable data) for the 50-day period following the respective start date of the season.

Figure 8: Subsurface and above-surface temperatures measured by vertical sections. (a) PVC tube with sensor cable wrapping prior to installation. (b) PVC tube temperature sensor (vertical section) installed within a dense conifer forest. Depth-time cross-section for (c) daily mean temperatures and (d) daily temperature range during 2013 snow melt period.

Geosci. Instrum. Method. Data Syst. Discuss., https://doi.org/10.5194/gi-2018-8
Manuscript under review for journal Geosci. Instrum. Method. Data Syst.
Discussion started: 23 March 2018
© Author(s) 2018. CC BY 4.0 License.

Geoscientific Instrumentation Methods and Data Systems Discussions
Open Access
EGU

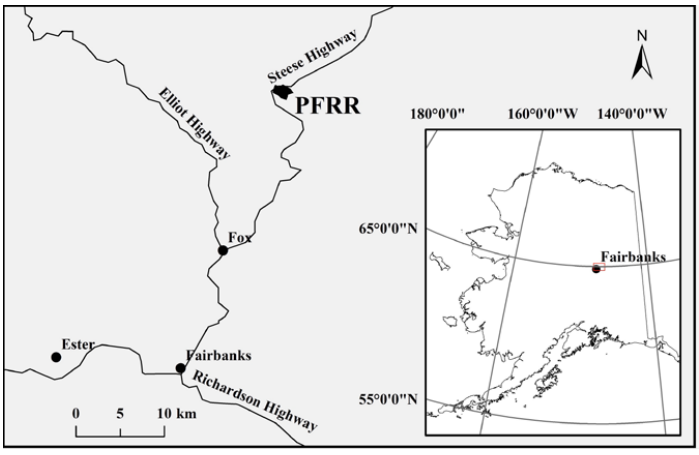

Fig01

Geosci. Instrum. Method. Data Syst. Discuss., https://doi.org/10.5194/gi-2018-8
Manuscript under review for journal Geosci. Instrum. Method. Data Syst.
Discussion started: 23 March 2018
© Author(s) 2018. CC BY 4.0 License.

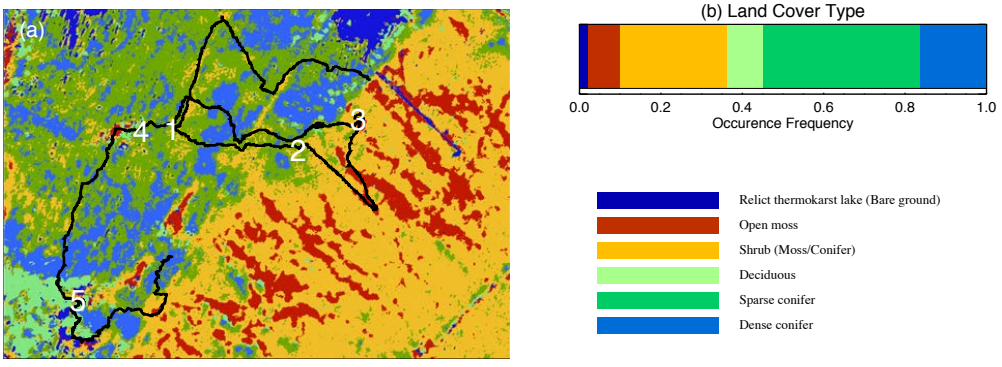

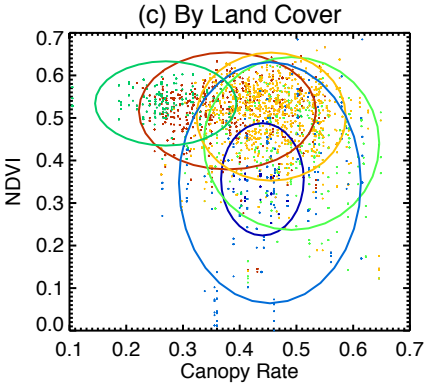

Fig02

Geosci. Instrum. Method. Data Syst. Discuss., https://doi.org/10.5194/gi-2018-8
Manuscript under review for journal Geosci. Instrum. Method. Data Syst.
Discussion started: 23 March 2018
© Author(s) 2018. CC BY 4.0 License.

Geoscientific Instrumentation Methods and Data Systems Discussions
Open Access
EGU

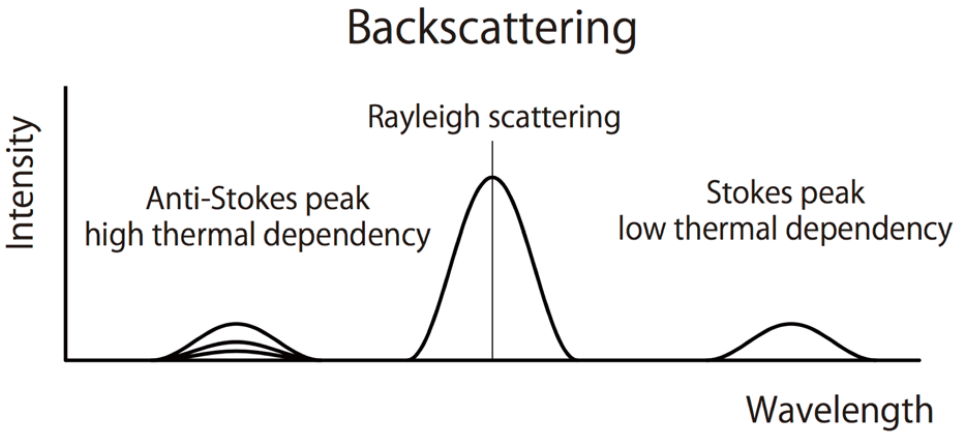

Fig03

Geosci. Instrum. Method. Data Syst. Discuss., https://doi.org/10.5194/gi-2018-8
Manuscript under review for journal Geosci. Instrum. Method. Data Syst.
Discussion started: 23 March 2018
© Author(s) 2018. CC BY 4.0 License.

Geoscientific Instrumentation Methods and Data Systems Discussions
Open Access
EGU

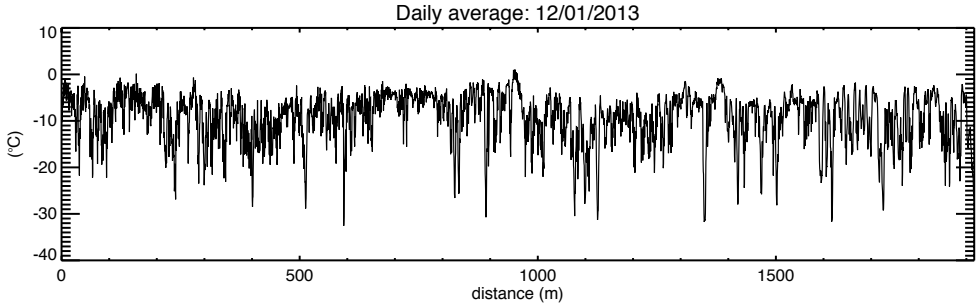

Fig04

Geosci. Instrum. Method. Data Syst. Discuss., https://doi.org/10.5194/gi-2018-8
Manuscript under review for journal Geosci. Instrum. Method. Data Syst.
Discussion started: 23 March 2018
© Author(s) 2018. CC BY 4.0 License.

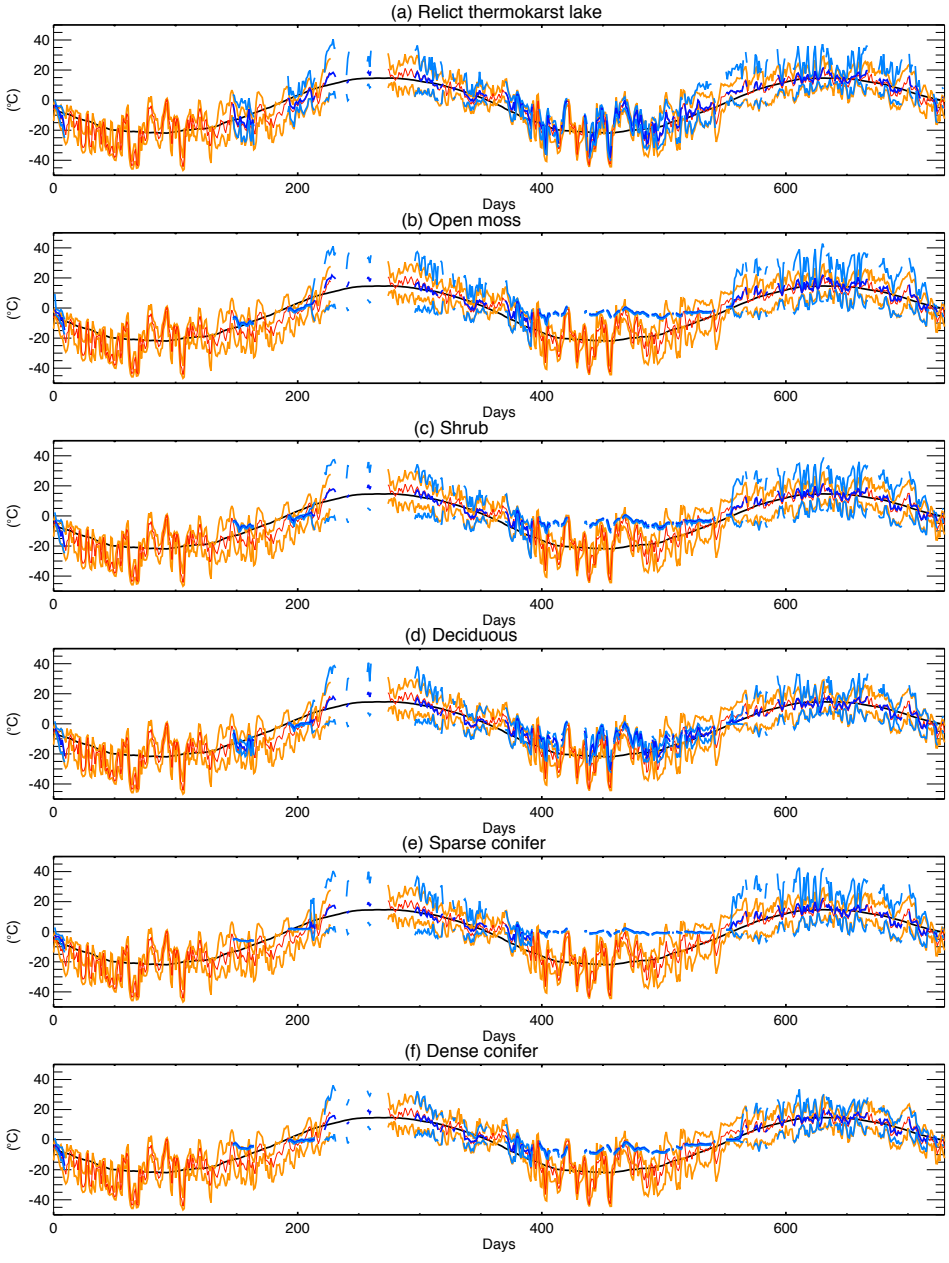

Fig05

Geosci. Instrum. Method. Data Syst. Discuss., https://doi.org/10.5194/gi-2018-8
Manuscript under review for journal Geosci. Instrum. Method. Data Syst.
Discussion started: 23 March 2018
© Author(s) 2018. CC BY 4.0 License.

Geoscientific Instrumentation Methods and Data Systems Discussions
Open Access
EGU

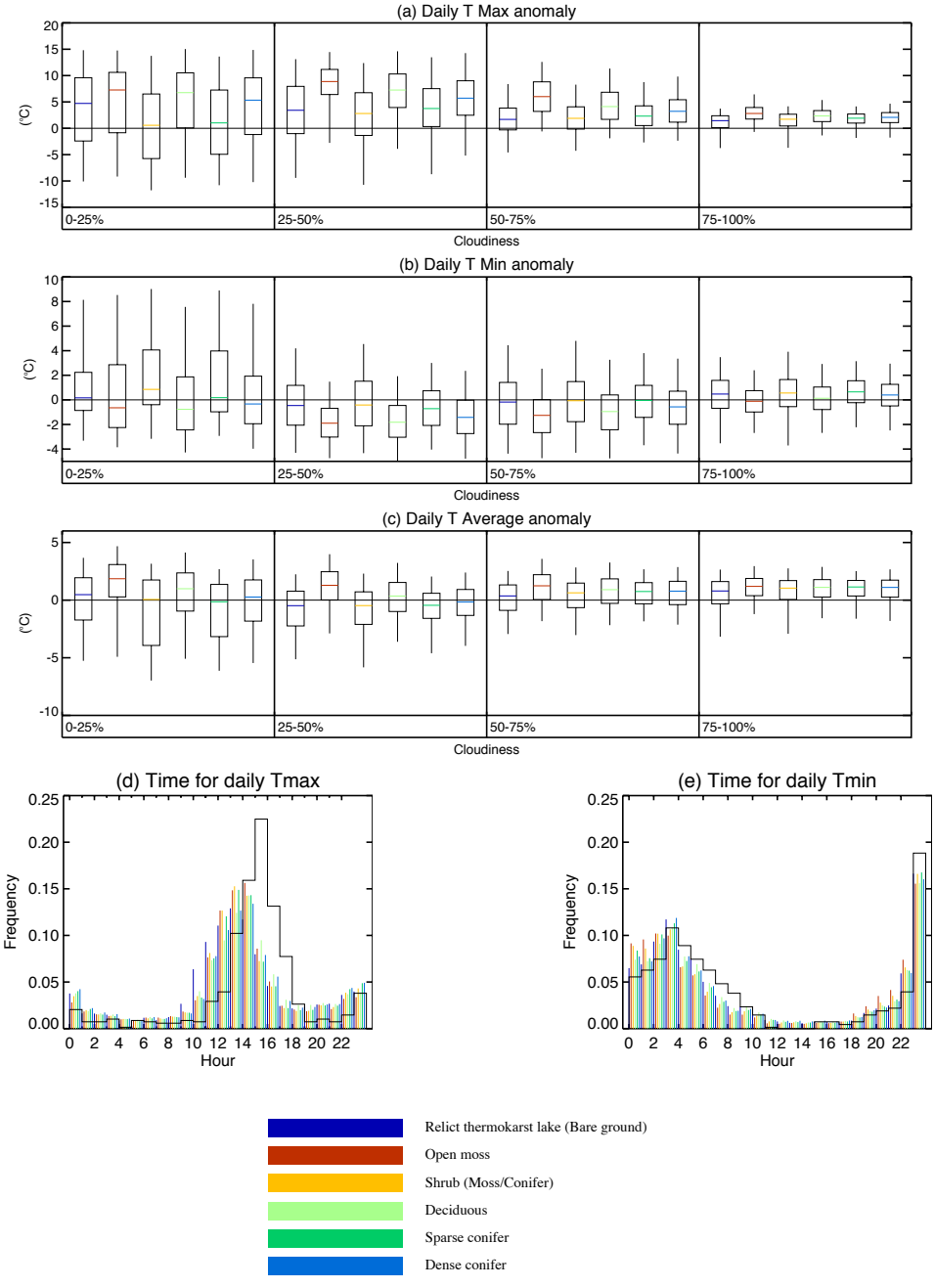

Fig06

Geosci. Instrum. Method. Data Syst. Discuss., https://doi.org/10.5194/gi-2018-8
Manuscript under review for journal Geosci. Instrum. Method. Data Syst.
Discussion started: 23 March 2018
© Author(s) 2018. CC BY 4.0 License.

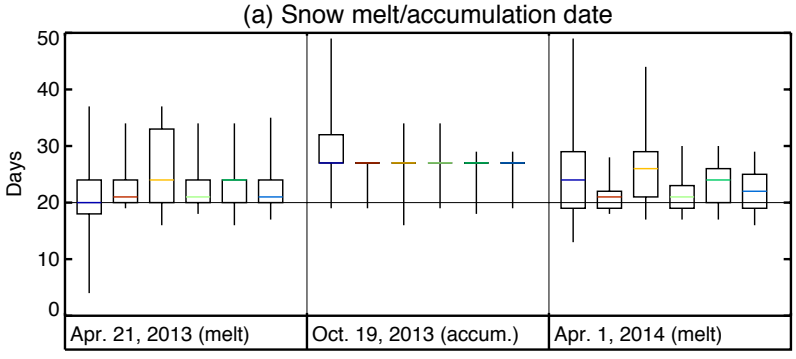

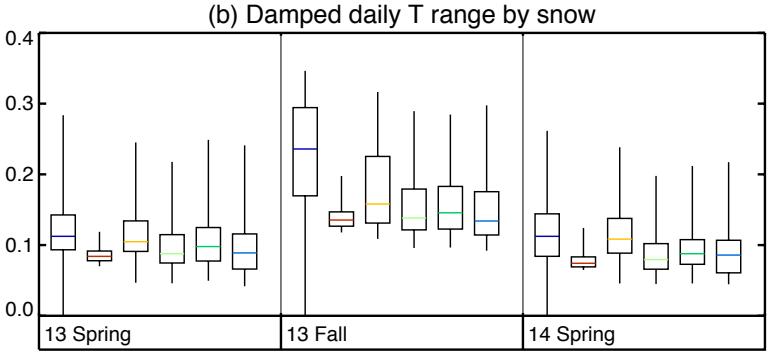

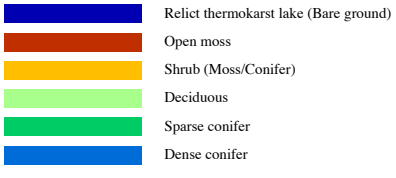

Fig07

Geosci. Instrum. Method. Data Syst. Discuss., https://doi.org/10.5194/gi-2018-8
Manuscript under review for journal Geosci. Instrum. Method. Data Syst.
Discussion started: 23 March 2018
© Author(s) 2018. CC BY 4.0 License.

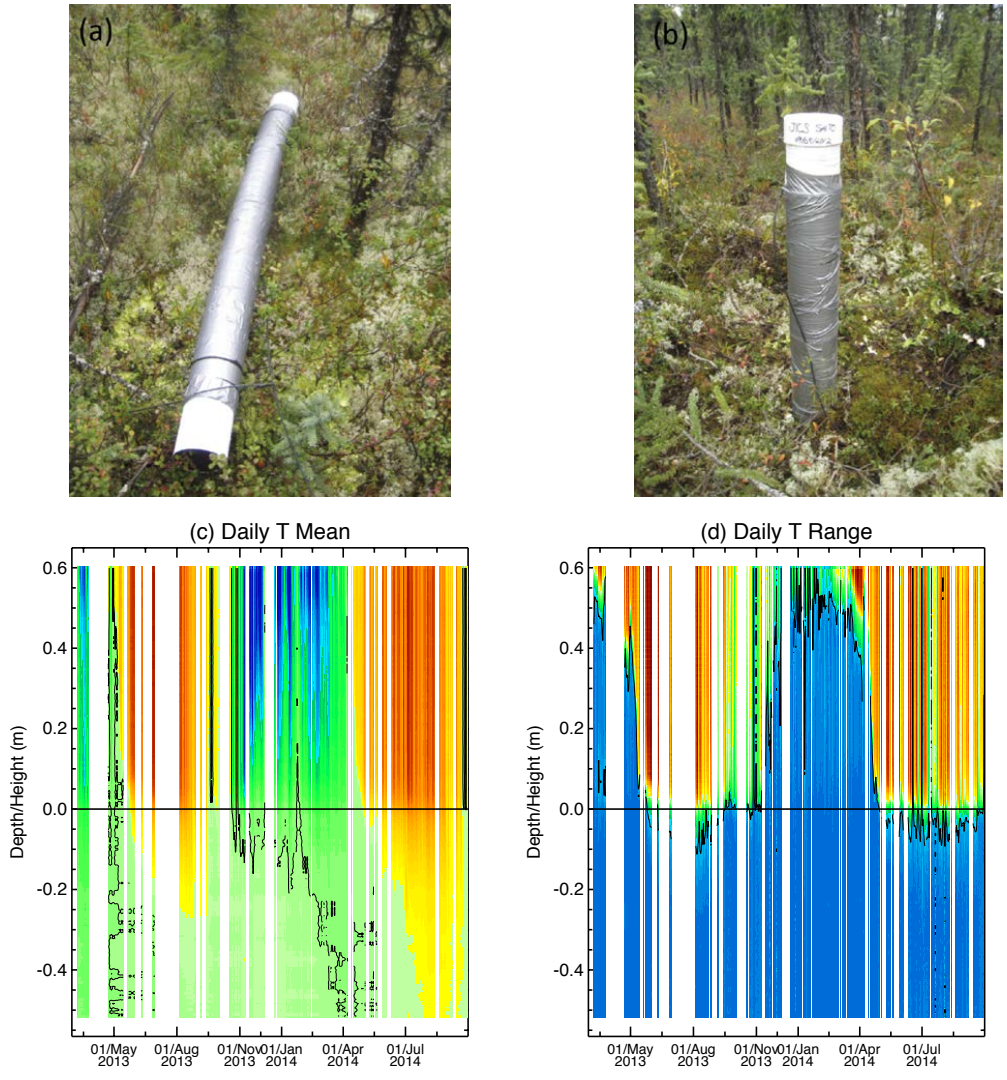

Fig08